COMPLEX MODES IN SHIELDED PLANAR MICROSTRIP LINES

Ching–Kuang C. Tzuang, Jen–Tsai Kuo, Ching–Cheng Tien,
Jiing–Shyue Jang, and Te–Hui Wang

Institute of Communication Engineering
National Chiao Tung University
Hsinchu, Taiwan, R.O.C.

ABSTRACT

This paper analyzes the existence of complex modes, which have important effects on the properties of planar transmission line discontinuities, in electrically shielded microstrip lines. A rigorous full–wave spectral domain approach (SDA) with a newly proposed and tested set of basis functions can efficiently and accurately determine the complex modes of a class of general planar transmission line problems if the complex modes exist. Under the case studies of this paper, it shows that the complex modes may exist in every shielded microstrip lines. Both convergence study and the cross–sectional field patterns, which guarantee the correct boundary conditions being satisfied, confirm the validity of the solutions for complex modes. Theoretical results for fundamental, higher order, evanescent, and complex modes are presented for symmetric coupled microstrip lines.

INTRODUCTION

The characterization of planar or quasi–planar transmission line discontinuities plays an important role for the computer–aided design (CAD) of millimeter–wave and microwave integrated circuits [1]. Without the knowledge of the complex modes in an electrically shielded enclosure, the analysis of a discontinuity problem might lead to inaccurate results. Omar and Schünemann [2] pointed out that the irregularity of the frequency response of the normalized input reactance of a finline discontinuity problem would exist if the complex modes associated with the finline were ignored. So far two methods to obtain the solutions of complex modes for microstrip and slotlines (or finlines) are reported. The singular integral equation techniques (SIE) have been efficiently applied to analyze symmetric finline [3] and microstrip [4] problems. The other is based on the SDA [5].

Notice that all the reported solutions of the complex modes are for **symmetric** transmission lines. The objective of this paper is to explore the possible existence of complex modes in **general** planar and quasi–planar microstrip lines based on the SDA.

We will briefly describe the basic features of the SDA and list the set of basis functions employed in the SDA with some explanations. Then, the theoretical results covering various interesting aspects are reported as follows.
1) The first fifteen or sixteen modes and mode conversions including fundamental, higher order, evanescent, and complex modes are presented for even and odd mode propagations of coupled microstrip lines.
2) The field patterns of the complex modes are investigated. Besides the assurance of the boundary conditions being satisfied, the physical implications are discussed.
3) The convergence study for the solutions of complex modes is performed.

Complex modes are found in suspended microstrip lines of various forms, too. Thus it is plausible to conclude that complex modes may exist in most shielded planar and quasi–planar transmission lines. In practice, their existences should not be overlooked since all the data reported in the paper have shown that the third or the fourth higher order modes may have already degenerated into complex modes.

FORMULATION

Spectral Domain Approach (SDA)

The spectral domain approach has been widely accepted for the analyses of numerous transmission lines regardless of whether they are open or close structures [6]. When analyzing stratified microstrip lines as shown in Fig.1, the SDA is even more attractive if the concept of the immitance approach is invoked [7]. Conceptually the immitance approach combines the network and field theories and results in much more physical insight than other techniques developed for microstrip and slotline analyses. For the convention shown in Fig.1, the SDA starts with the Fourier transform defined as follows.

$$\int_{-\infty}^{\infty} f(x,y)\cdot e^{j\alpha x}\cdot dx = \tilde{f}(\alpha,y) \qquad \text{Eq.(1)}$$

By the immitance approach [7], the dyadic Green's function can be derived, i.e.,

$$\begin{bmatrix} \tilde{Z}_{zz}(\gamma) & \tilde{Z}_{zx}(\gamma) \\ \tilde{Z}_{xz}(\gamma) & \tilde{Z}_{xx}(\gamma) \end{bmatrix} \begin{bmatrix} \tilde{J}_z \\ \tilde{J}_x \end{bmatrix} = \begin{bmatrix} \tilde{E}_z \\ \tilde{E}_x \end{bmatrix} \qquad \text{Eq.(2)}$$

,where γ is the propagation constant.

After matching the final boundary conditions imposed on the metal–dielectric interface a nonstandard eigenvalue problem can be formulated, namely,

$$\det\left(G_{n\times n}(\gamma)\right) = 0 \qquad \text{Eq.(3)}$$

where $\gamma=\alpha+j\beta$, and $e^{-\gamma z+jwt}$ factor is assumed. The roots of Eq.(3) are the propagation constants (γ's) for propagating, higher order, evanescent, and complex modes.

CH2725-0/89/0000-0495$01.00 © 1989 IEEE

Preconditioned Basis Functions in SDA

Jansen [8] listed six criteria for obtaining the basis functions used in SDA, namely, (1) edge condition, (2) twice continuous differentiability, (3) completeness, (4) integral relationship between longitudinal and transverse currents of the microstrip line, (5) ability to represent nearly true modal current distributions, and (6) capability of being Fourier transformed. The longitudinal and transverse currents are derived according to the above criteria, namely

$$J_z(x) = \sum_{m=1}^{2} \sum_{n=1}^{N} a_n^m \, j_{zn}^m(x), \quad \text{and}$$

$$j_{zn}^{1,2}(x) = (1 \pm x)^{\frac{n}{2}-1} \qquad \text{Eq.(4)}$$

$$J_x(x) = \sum_{m=1}^{2} \sum_{n=1}^{N} b_n^m \, j_{xn}^m(x), \quad \text{and}$$

$$j_{xn}^{1,2}(x) = (1 \pm x)^{\frac{n}{2}} - \sqrt{2}\,(1 \pm x)^{\frac{n+1}{2}} + (1 \pm x)^{\frac{n+2}{2}}/2 \qquad \text{Eq.(5)}$$

where superscripts 1, 2 correspond to the edge conditions in terms of normalized space coordinate at x=1 and −1, respectively.

Many symmetric and asymmetric microstrip lines have been investigated by employing this newly proposed set of basis functions shown in Eqs.(4–5). No spurious solution has been found. The modal longitudinal and transverse currents reported in Fig. 5 and Fig. 6 of previous paper [10] agree very well with current approach.

In addition, the point–matching technique has been adopted into the SDA with the incorporation of Eq. (4) and Eq. (5). It is clear from Table 1 that as N increases, fewer number M of point–matching intervals [10] is required for the solution of one of a pair of complex modes to converge. The case of N=3 and M=4 results in a solution for complex modes that would be obtained by N=1 and M=20. Likewise, the cases of N=3, M=20 and N=7, M=4 have very close solutions.

Since the accuracy of the modal solutions has been established, the solutions reported hereafter use N=3, M=0.

Table. 1 Convergence test for the solution of a complex mode in a shielded symmetric microstrip line. Enclosure: 12.7mm × 12.7mm, f=15 GHz, w=1.27mm, ϵ_r=20, h_1=1.27mm.

N†	M*	$(\beta,-\alpha)/\kappa_o$‡
1	4	(0.065840710,–1.0194247)
	8	(0.065589305,–1.0195825)
	20	(0.065551491,–1.0196082)
3	4	(0.065552678,–1.0196089)
	8	(0.065550246,–1.0196104)
	20	(0.065546229,–1.0196135)
5	4	(0.065550087,–1.0196116)
	8	(0.065546116,–1.0196154)
	20	(0.065537774,–1.0196240)
7	4	(0.065544846,–1.0196181)
	8	(0.065537462,–1.0196332)
	20	(0.065521697,–1.0196442)

† The order of SDA basis functions for analysis.
* The number of equally spaced intervals.
‡ Normalized propagation constant $\gamma/\kappa_o=(\alpha+j\beta)/\kappa_o$.

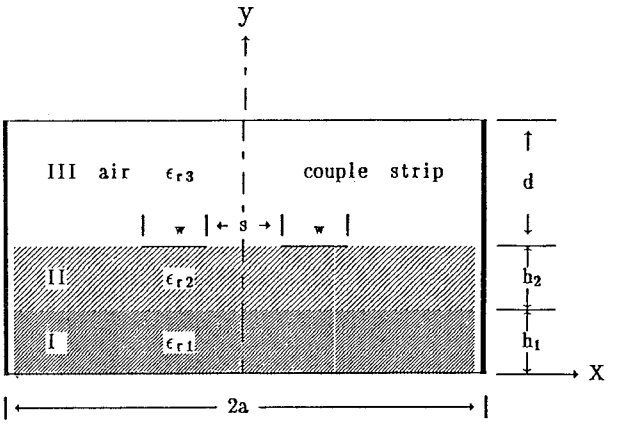

Fig.1 Cross–sectional view of coupled microstrip lines with stratified dielectric layers.

RESULTS

Fundamental, higher order, evanescent, and complex modes in general microstrip lines

The modal solutions shown in Fig. 2–(a) and Fig. 2–(b) compare the results of the normalized propagation constants obtained by SDA and those by SIE [4] for a symmetric microstrip line, respectively. Only even mode data are shown here. The fundamental mode is designated as 1, first higher order mode 2, and so on. Reading from the right hand side of the figures, the unprimed number is the mode before conversion and the order of primed number denotes the frequency of mode conversions. Both figures agree generally except that mode 7 of Fig. 2–(a) becomes evanescent quickly in the neighborhood of 22.5 GHz and modes 5 and 8 of Fig. 2–(b) were missed. Mode 10 of Fig. 2–(a) contributes to another complex modes that were not reported previously. Before modes 4 and 6 degenerate into complex modes, a small backward wave region exists as shown in Fig. 2–(a). Modes 8 and 9 also split into complex modes. Immediately after modes 8' and 9' lead into evanescent modes, mode 9' and mode 10 form another complex modes. The validity of every mode reported in Fig. 2–(a) has been checked by cross–sectional electric and magnetic field patterns to ensure that the correct physical solution has been found. One of the advantages of using the modified SDA is the fact that the odd mode propagation constants can be obtained simultaneously. Fig. 2–(c) illustrates the results for odd mode propagation. There is no limitation of the approach to analyze the asymmetric microstrip lines.

Fig. 3–(a) and Fig. 3–(b) are modal solutions for odd mode and even mode propagations of coupled microstrip lines, respectively. The distributions of complex modes are more complicated than data shown in Fig. 2–(a) or Fig. 2–(b) of a symmetric microstrip line. Many mode conversions occur in these figures. In Fig. 3–(a), for instance, modes 10 and 13 and modes 7 and 11 degenerate into complex modes. These complex waves convert to evanescent modes designated as 10', 13', 7', and 11'. Again modes 10' and 13' degenerate into complex modes and are back to evanescent modes 10" and 13". Modes 10" and 12 and modes 13" and 7' degenerate into complex modes. They are finally back to evanescent modes designated as 10"', 12', 13"', and 7".

Similarly Fig. 3–(b) indicates the fact that many regions consisting of complex modes and mode conversions occur frequently.

Field patterns for complex modes

For the situation that modal solution is either real (evanescent) or imaginary (propagating), the field patterns of this case are polarized in linear sense. The complex modes, on the other hand, are polarized in elliptical sense since the field amplitudes are complex in nature. Fig. 4–(a), (b), (c) and (d) are the plots of odd–symmetric electric field patterns of one of the complex modes at different locations along z–axis, i.e. z=0, $2\pi/4\beta$, $2\times2\pi/4\beta$ and $3\times2\pi/4\beta$, when the electric field patterns are observed instantly at t=0. Only part (one fifth) of the field patterns from bottom enclosure are plotted for better illustrations for field near metallic strips. Each plot represents the relative amplitude nomalized to itself. The transverse electric displacement vector $\mathbf{D}_t=\epsilon_r\mathbf{E}_t$ is much stronger underneath the dielectric–air interface. The field distribution is HE_{61} type. The influence of side walls and bottom enclosure on the field patterns is clear. The field patterns are denser in the regions other than metallic strips.

CONCLUSION

The existences of complex modes together with backward waves are shown to exist in both symmetric microstrip line and coupled microstrip lines. Mode charts of the propagation constant as a function of frequency illustrate the fact that complex modes may exist over most frequency spectrum of interest. In addition, the third or fourth higher order modes may start to degenerate into complex modes for all the case studies presented. Not being reported in the paper, the suspended symmetric and asymmetric microstrip lines also have complex modes. Therefore it is important not to ignore the existence of complex modes associated with most planar microstrip lines incorporated in MMIC or hybrid MIC designs.

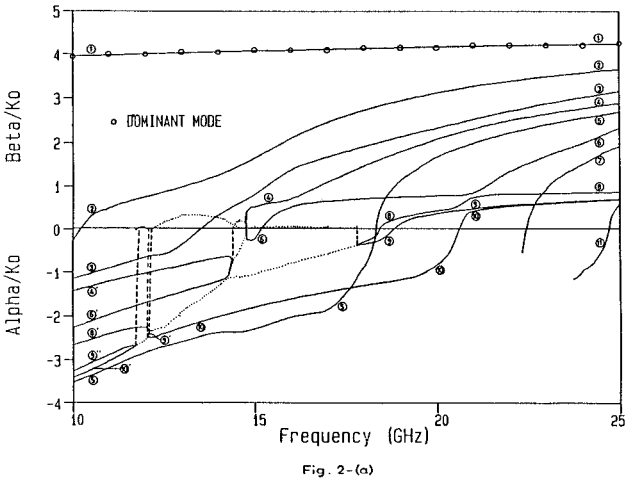

Fig. 2-(a)

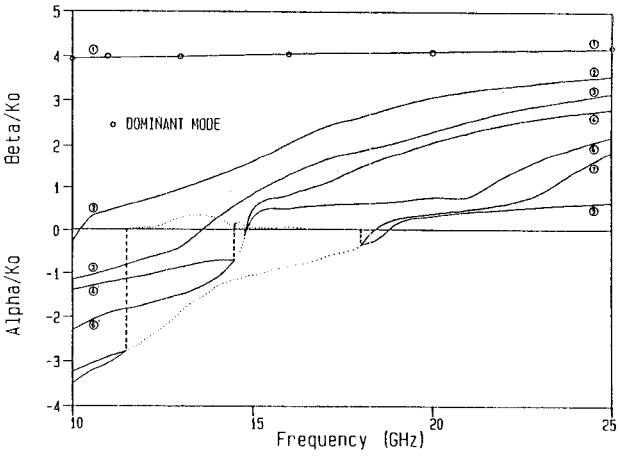

Fig. 2-(b)

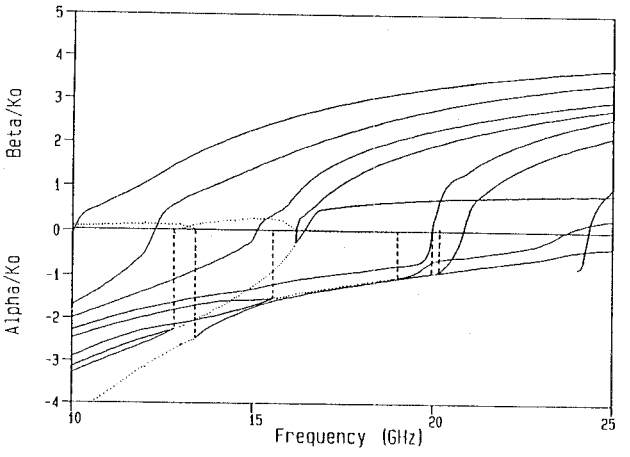

Fig. 2-(c)

Fig.2 Normalized propagation constant $\gamma=\alpha+j\beta$ versus frequency. (a) The improved SDA solutions for even mode propagations. (b) The SIE solutions for even mode propagations. (c) The improved SDA solutions for odd mode propagations.2a=12.7mm,s=0, 2w=h1+h2=1.27mm, $\epsilon_{r1}=\epsilon_{r2}=20$, $\epsilon_{r3}=1$, d+h1+h2= 12.7mm.

REFERENCES

[1] N.H.L. Koster and R.H. Jansen, *IEEE Trans.* Vol. MTT– 34, No. 2, pp.213–223, Feb. 1986.

[2] A.S. Omar and K.F. Schünemann, *IEEE Trans.* Vol. MTT– 34, No. 12, pp.1508–1514, Dec. 1986.

[3] A.S. Omar and K.F. Schünemann, *IEEE Trans.* Vol. MTT– 33, No. 12, pp.1313–1322, Dec. 1985.

[4] W.–X. Huang and T. Itoh, *IEEE Trans.* Vol. MTT–36, No. 1, pp.163–165, Jan. 1988.

[5] C.J. Railton and T. Rozzi, *IEEE Trans.* Vol. MTT–36, No. 5, pp.865–874, May. 1988.

[6] R.H. Jansen, *IEEE Trans.* Vol. MTT–33, No. 10, pp.1043–1056, Oct. 1985.

[7] T. Itoh, *IEEE Trans.* Vol. MTT–28, No. 7, pp.733–736, Jul. 1980.

[8] R.H. Jansen, *IEEE Trans.* Vol. MTT–26, No. 2, pp. 75–82, Feb. 1978.
[9] M. Kobayashi and F. Ando, *IEEE Trans.* Vol. MTT–35, No. 2, pp.101–105, Feb. 1987.
[10] N. Faché and D.D. Zutter, *IEEE Trans.* Vol. MTT–36, No. 4, pp.731–737, Apr. 1988.

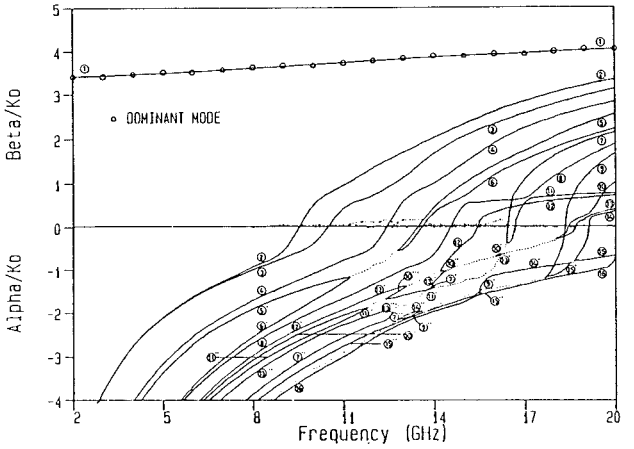

Fig. 3-(a)

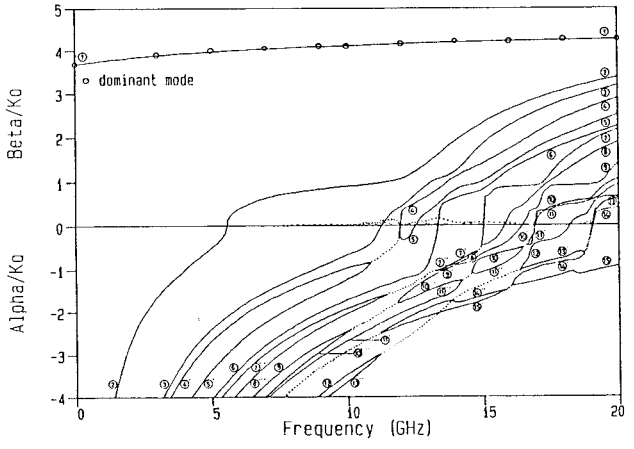

Fig. 3-(b)

Fig.3 Normalized propagation constant $\gamma/\kappa_0 = (\alpha+j\beta)/\kappa_0$ of coupled microstrip lines versus frequency. The dimensions of the coupled microstrip lines are shown in Fig.1. (a) The odd mode propagation. (b) The even mode propagation. Parameters: 2a=25.4mm, s=1.27mm, w=1.27mm, d+h1+h2=12.7mm, h1+h2=1.27mm, $\epsilon_{r1}=\epsilon_{r2}=20$, $\epsilon_{r3}=1$.

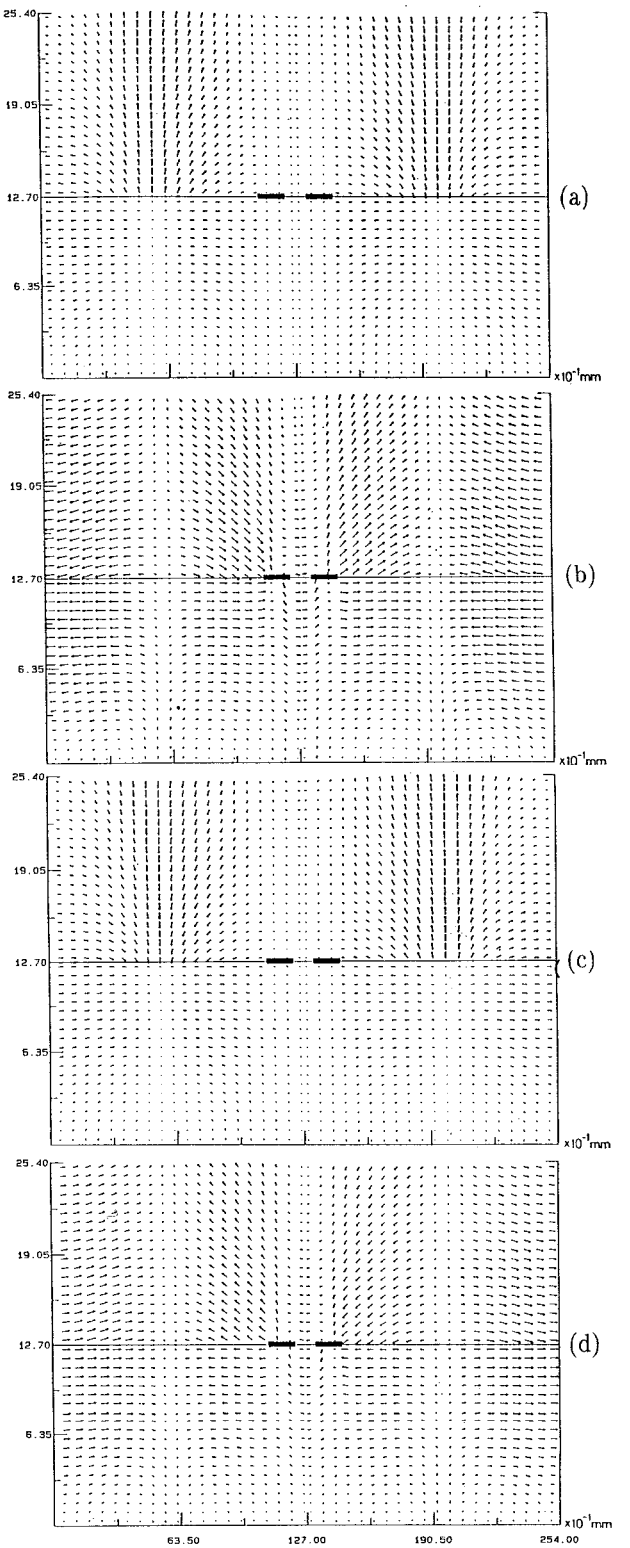

Fig.4 Odd mode electric field patterns for one of the complex modes of the coupled microstrip lines. f=15GHz. $\gamma = \alpha+j\beta = 0.883976 + j0.048256$. $\omega t=0$. (a) $\beta\ell=0$, (b) $\beta\ell=\pi/2$, (c) $\beta\ell=\pi$, (d) $\beta\ell=3\pi/2$.